Experimental Investigation of Droplet Injections in the Vicinity of the Critical Point

Florian Weckenmann*[1], Benjamin Bork[2], Grazia Lamanna[1], Andreas Dreizler[2] and Bernhard Weigand[1]
[1] Institut für Thermodynamik der Luft und Raumfahrt (ITLR), Universität Stuttgart, Pfaffenwaldring 31, 70569 Stuttgart, Germany
[2] FG Reaktive Strömungen und Messtechnik, Maschinenbau/Centre of Smart Interfaces, TU Darmstadt, Jovanka-Bontschits-Straße 2, 64287 Darmstadt, Germany
Florian.Weckenmann@itlr.uni-stuttgart.de | Fax: +49 (711) 685-62317

ABSTRACT

One of the key parameters for an efficient and stable combustion is the disintegration process of the injected liquid fuel. The complex interdependency between evaporation, mixing and droplet dynamics makes it difficult to describe this problem numerically or with an analytical model. Additionally, if the pressure and temperature inside the combustion chamber reach or even exceed the critical point of the injected fuel, standard evaporation models fail completely. In order to gain more insight into the physical processes during such a fuel injection into a supercritical environment, the complexity is reduced. In a first step, the behaviour of an isolated droplet, injected into supercritical chamber conditions, needs to be fully understood. In this context, the term supercritical refers to the critical point of the injected fluid. In a next step, droplet chains and finally entire fuel sprays will be investigated. The ultimate goal of this work is the understanding and modelling of the fundamental processes of fuel disintegration and mixing into a supercritical atmosphere.
An extensive experimental investigation of droplet injections at different pressures and temperatures, even above the critical point of the injected fluid, is presented. The acetone droplet can be preheated up to 89% of the critical temperature. The nitrogen atmosphere can be adjusted to reduced values of $T_{injection}/T_{critical}$ =1.03 and $p_{injection}/p_{critical}$ = 1.27 with respect to the injected fuel. The focus of the experiments lies in assessing the dynamics and evaporation rate (when applicable) of the falling droplet. Due to the presence of strong oscillations, novel 3D volume reconstruction methods are applied in an attempt to enable an accurate estimation of the evaporation rate from 2D shadowgraphy images. The droplet size, oscillation and evaporation, especially in the wake of the falling droplet, are discussed. Finally, a first attempt to evaluate the influence of the temperature and pressure on the evaporation rate, up to the vicinity of the critical point, is made.

INTRODUCTION

The investigation of droplet injections close to the critical point is of interest for various technical applications, e.g. modern diesel engines, gas turbines and rocket engines. In order to increase the efficiency and reduce the emission of pollutants the trend is towards higher temperatures and pressures inside combustion chambers. This may result in supercritical chamber conditions with respect to the injected fuel. Hence standard evaporation models have to be checked upon their validity at these conditions. The situation becomes even more complicated if the fuel, initially at subcritical temperature, becomes supercritical after injection. Supercritical anomalies not only make the analysis and modelling extremely challenging [1], but also strongly affect the evaporation/emission process. In the following the

term “evaporation” will be used for subcritical conditions, whereas the term “emission” will be used for supercritical conditions. Especially in the vicinity of the critical point thermodynamic properties can change drastically. While the surface tension, heat of vaporisation and viscosity decrease rapidly towards the critical point, the isothermal compressibility and heat capacity (c_v and c_p) are increased. In order to validate numerical simulations and develop new models for supercritical droplet injections, experimental data are indispensable. In contrast to spray experiments, isolated droplet investigations reduce the complexity and enable very reproducible test conditions. Both aspects represent key prerequisites for gaining an understanding of the fundamental physical phenomena.

Many investigations have focused on the study of hanging droplets, either in micro-gravity or normal gravity, in quiescent surroundings or moving air [2 - 5]. Since the anchoring of the droplet at the capillary requires some value of surface tension, an observation of the transition from sub- to supercritical state is precluded in advance. A different approach was followed by Stengele et al. [7] who examined free falling one- and two component pentane and nonane droplets. The experimental setup could be pressurized and heated up to supercritical chamber conditions, with respect to the injected fluid. Droplet size and velocity were measured at different falling distances. The initial droplet size, chamber pressure and temperature were varied but a transition to a supercritical state has never been reached, most probably due to a relatively low injection temperature of 370 – 400 K ($T_{injection}/T_{critical}$ = 0.78) .

The goal of this work is the investigation of free falling droplets, injected at a temperature level closer to the critical temperature (up to $T_{injection}/T_{critical}$ = 0.89). The project is incorporated into the collaborative research centre SFB-TRR 75 which has the objective to gain a deeper physical understanding of the essential processes of droplet dynamics at extreme conditions [8]. The research centre enables a comprehensive experimental and numerical investigation and promotes the exchange of data and knowledge between the different projects.

A novel experimental setup has been developed, which enables a reliable droplet generation and detachment even at supercritical chamber conditions [9]. In this context the term “supercritical“ refers to the critical point of the injected fluid. The goal of the project is the fundamental understanding of the physical processes of supercritical droplet injections. Experimental data will be provided to support the development of droplet evaporation/emission models up to the critical point and beyond. The data will also be used for the validation of numerical simulations.

The droplets are analysed with different optical measurement techniques. Standard techniques like shadowgraphy or laser induced fluorescence (LIF) are employed. Additionally novel optical measurement techniques like planar laser induced fluorescence and phosphorescence (PLIFP) [10, 11] or differential infrared thermography (DIT) [12] are developed and evaluated.

The focus of this paper lies on the one hand on the evaluation of the shadowgraphy technique. In this context a phenomenological investigation of the droplet disintegration as a function of the chamber pressure and temperature has been carried out. First results of a novel 3D volume reconstruction algorithm will be presented, which allow for a more accurate calculation of the droplet size. An evaluation of the technique and the future range of application are discussed. On the other hand a thermodynamic analysis of droplet injections into supercritical chamber conditions is presented. Thermodynamic simulations of the system acetone/nitrogen in combination with the diffuse light technique prove to be an effective instrument for a first analysis of the possible transition from sub- to supercritical state.

MATERIALS AND METHODS

An experimental setup has been developed to investigate droplet injections in the vicinity of the critical point. The droplet chamber is made of a massive metal block consisting of highly temperature resistant steel. The temperature inside the chamber can be controlled with four vertically and two horizontally mounted heat cartridges. Optical access is granted with synthetic Quartz windows from four sides. A picture of the 3 D cross-section of the pressure chamber is displayed in Figure 1. The chamber was pressure tested up to 85 bar and can withstand temperatures up to 550 K. A droplet generator inlet is mounted at the lid. The droplet generator has been developed especially for high temperature and pressure conditions. Two copper electrodes are mounted on opposing sides, surrounding a steel capillary with an outer diameter of 0.7 mm. An inhomogeneous electric field is established between the electrodes and the capillary. The electric polarisation of the suspended droplet, due to the onset of the electric field, results in an electric force in downward direction. This artificial disturbance leads to a controlled detachment of the droplet. The benefits of this method lie in the great reliability and reproducibility of the detachment process even at high chamber pressures and temperatures. Great precautions are taken to avoid any residual charges on the droplet after detachment. The inlet itself has a recirculating oil cycle to control the temperature of the injected fluid separately. For more detailed information the reader is referred to [9].

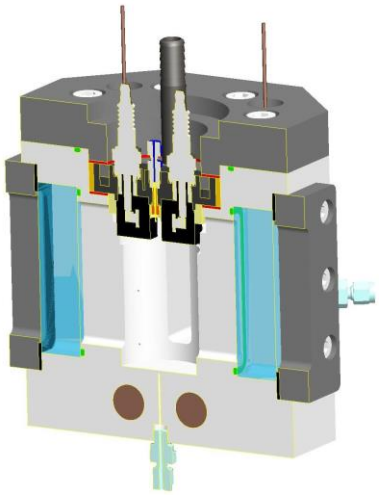

Figure 1: 3D cross-section of the droplet chamber

The gas atmosphere inside the droplet chamber consists of pure nitrogen. The injected fluid is acetone, which was chosen because of its moderate critical values and spectroscopic properties. The critical values of acetone are p_c = 47 bar and T_c = 508 K.

RESULTS

An extensive parametric study of free falling droplets from sub- to supercritical conditions has been conducted. In Table 1 a matrix with experimental test conditions is given. T_{ch} and p_{ch} refer to the chamber pressure and temperature, respectively. T_r and p_r are the reduced values, which are defined as T_{ch}/T_c (respectively p_{ch}/p_c). T_c and p_c are the critical temperature and pressure of the injected acetone. The initial temperature of the droplets, prior to detachment, was set equal to the chamber temperature for all experiments, except for the investigations at supercritical chamber conditions. For these experiments the temperature of the droplet was set to T_{inj} = 453 K (T_r = 0.89). The slightly subcritical temperature still allows the creation and anchoring of the droplet at the capillary. Pressure, temperature and composition of the surrounding gas have a great impact on the disintegration process of the falling droplet. Additionally, the initial temperature of the droplet prior to injection plays a major role especially in the vicinity of the critical point. The influence of chamber pressure can be seen in Figure 2 at the first four images. Each image is a compilation of snapshots of the same experiment at different times. The background of the images was normalized by subtracting a calibration image without injection. The experiments were conducted at constant chamber and

droplet temperature of 293 K. The chamber pressure was varied from 1 to 60 bars, see Figure 2. The increase in pressure had only minor effects on the droplet size and evaporation rate, but strongly influenced the falling process e.g. droplet velocity and oscillation. In order to gain more insight into the actual behaviour of the falling droplets a second test campaign with increased magnification and resolution was conducted.

Table 1 : Matrix of the experimental test conditions

p_{ch}/T_{ch}	293 K (T_r=0.58)	373 K (T_r=0.73)	473 K (T_r=0.93)	523 K (T_r=1.03)
1 bar (p_r=0.02)	X			
20 bar (p_r=0.42)	X	X		
40 bar (p_r=0.85)	X	X	X	
60 bar (p_r=1.27)	X	X	X	X (T_{inj} = 453 K)

The oscillations, which can be seen in the magnified picture in Figure 2 at the right, increase in magnitude with falling distance. In Figure 3 two experiments at 60 bar and increasing chamber and injection temperature are compared. The disintegration process gains dynamic due to the strong evaporation, flow convection within the droplet chamber and lower surface tension of the acetone droplet. The initial droplet size decreases with increasing temperature due to the lower surface tension of the acetone [9]. In the wake of the falling droplet a Schlieren system, consisting of a dense acetone-rich gas mixture, can be seen. With rising chamber and injection temperature these structures can no longer be distinguished from the liquid acetone droplet and no clear droplet boundary can be identified. On the right hand side of Figure 3 a droplet injection at supercritical chamber conditions, with respect to the injected acetone, is shown. The droplet was preheated to 89% of the critical temperature. A detailed analysis of the droplet behaviour at those conditions is given in the second part of the results section.

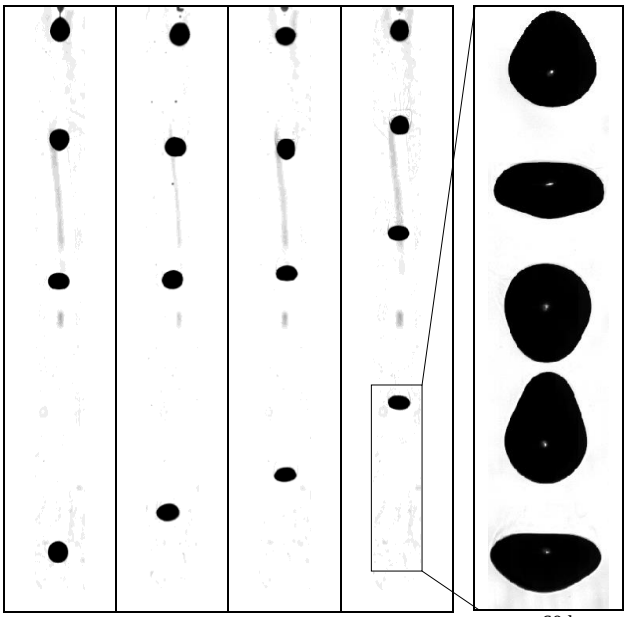

p_{ch} = 1 bar T_{ch} = 293 K T_{inj} = 293 K | p_{ch} = 20 bar T_{ch} = 293 K T_{inj} = 293 K | p_{ch} = 40 bar T_{ch} = 293 K T_{inj} = 293 K | p_{ch} = 60 bar T_{ch} = 293 K T_{inj} = 293 K | p_{ch} = 60 bar T_{ch} = 293 K T_{inj} = 293 K

Figure 2: Pressure dependency

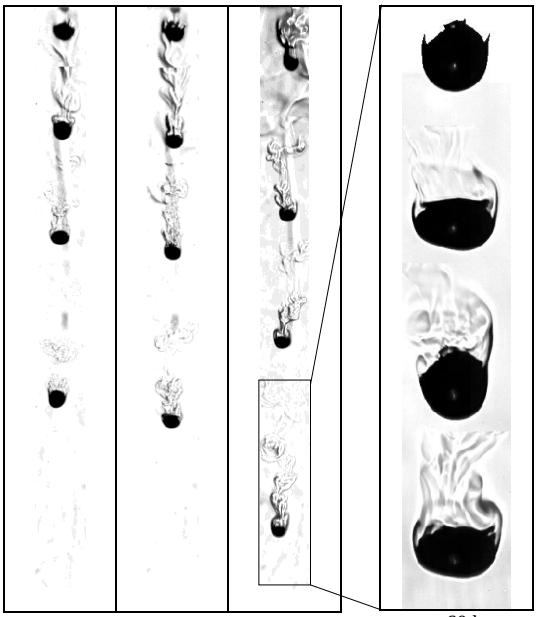

p_{ch} = 60 bar T_{ch} = 373 K T_{inj} = 373 K | p_{ch} = 60 bar T_{ch} = 423 K T_{inj} = 423 K | p_{ch} = 53 bar T_{ch} = 523 K T_{inj} = 453 K | p_{ch} = 60 bar T_{ch} = 523 K T_{inj} = 453 K

Figure 3: Temperature dependency

The strong oscillations and the uncertainty about the droplet contour, hinder the exact calculation of the droplet diameter. The algorithm to calculate the droplet volume relies on the assumption of axis symmetry around the falling axes. This is not always satisfied especially for high chamber temperatures and pressures [9]. In order to solve this problem a novel 3D reconstruction algorithm, adapted from Kim and Park [13] has been employed. It relies on the simultaneous recording of the falling droplet from two different sides with an angle of 90°, illustrated in Figure 4. The image is captured with a single CCD camera and focusing lens. This approach has the benefit of an automatic time synchronisation and the same magnification for both images. Both light paths are directed to the camera via mirrors and travel the same distance. Finally after post processing these images the contour of the two droplets can be reconstructed to a 3D droplet shape and volume. The algorithm is able to estimate the volume and area of objects within ±6% and ±4% error, respectively. For a more detailed description of the algorithm, including error analysis, the reader is referred to [13]. In Figure 5 and Figure 6 the droplet size history with the standard method, assuming axis symmetry, and the novel 3D volume reconstruction method are compared, using the experiments, depicted in Figure 2. For both evaluations the initial droplet diameter decreases only slightly with increasing pressure. The diameter reduction, caused by evaporation, can be neglected at these low temperature conditions. In Figure 5 the assumption of axis symmetry with the falling axes is not valid at all times and leads to a fluctuation of the derived volume. The general trend of small evaporation rates at moderate temperature is still captured. The uncertainty with this method is at most 0.26 mm in diameter which makes it impossible to determine evaporation rates in the same order of magnitude. In Figure 6 the results of the new 3D reconstruction

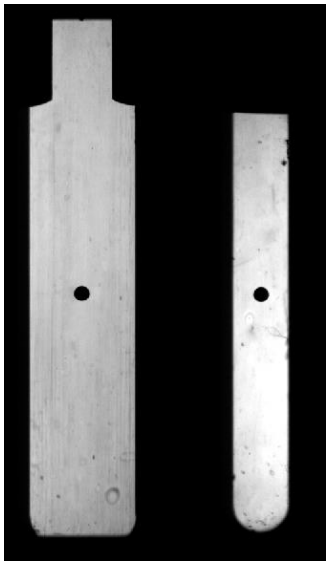

Figure 4 : Image alignment for 3D volume reconstruction

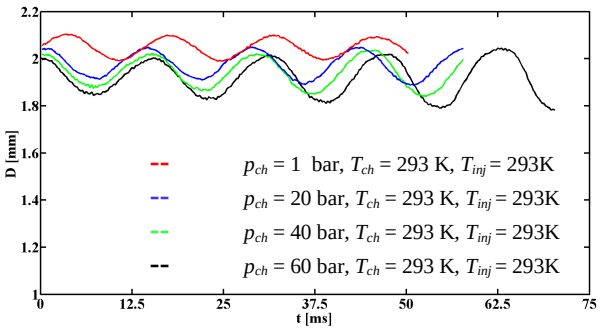

Figure 5: Droplet size history with axis symmetry

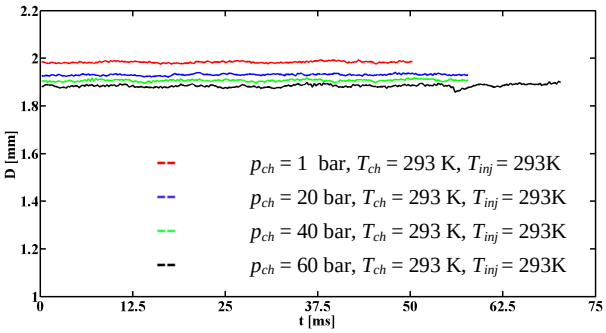

Figure 6: Droplet size history with 3-D algorithm

method for the same experiments are displayed. The uncertainty is at most 0.045 mm in diameter and has a standard deviation of 0.006 mm. This enables a more precise estimation of the actual evaporation rate. The accuracy can be further improved by reducing the Field of View (FOV), which results in a better spatial resolution. The next step will be the adaption of the algorithm to high temperature conditions.

Both methods for the evaluation of the droplet size history rely on the accurate detection of the droplet boundary. For high temperature conditions it becomes increasingly difficult to capture the droplet surface on shadowgraph images, see Figure 3. The dense acetone rich gas

mixture, surrounding the droplet especially in its wake, changes the refractive index and can no longer be distinguished from the liquid droplet. For the measurement at high temperature conditions, complementary optical techniques, e.g. Rayleigh scattering, might help to detect the phase boundary more precisely. On condition that the contour can be provided with these methods a calculation of the evaporation/emission rate even close to the critical temperature seems feasible.

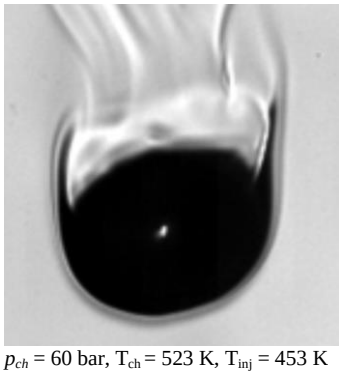

p_{ch} = 60 bar, T_{ch} = 523 K, T_{inj} = 453 K
Figure 7: Supercritical droplet Injection

The situation gets even more complicated for experiments at supercritical chamber conditions with respect to the injected acetone (p_{ch} > 47 bar, T_{ch} > 508 K). The boundary becomes more diffuse and finger-like ligaments are formed at the top part of the droplet, see Figure 7. Different assumptions on the nature of these ligaments have been made, e.g. consisting of liquid acetone or sub- or supercritical acetone rich gas mixtures. To check these theories the behaviour and disintegration process of the droplet itself was investigated. Special attention was given to open questions, such as the possible transition of the droplet from sub- to supercritical state during free fall. The investigation of these phenomena followed different approaches. The first analysis focused on the magnified shadowgraphy images, displayed in Figure 3 (right) and Figure 7. The ligaments can be witnessed at different falling positions and droplet velocities. Furthermore the upper part of the droplet, between the ligaments, shows a diffuse boundary between the acetone droplet and the surrounding gas. The lower boundary of the droplet appears sharper, which can be attributed to the flow convection around the droplet. During the entire falling process the droplet oscillates, which suggests that the surface tension of the droplet has not vanished completely. This behaviour leads to the assumption that at least the inner core of the droplet is at a subcritical state. The second investigation focused on the ligaments itself. A different illumination technique, the diffuse lighting method, was applied. In contrast to the shadowgraphy images, this method is more sensitive to phase boundaries and might be able to serve as a marker for a liquid state. Highly incoherent light, produced by a milk glass, illuminates the capillary and the droplet from different directions. An example of an image captured with this technique can be seen in Figure 8. Although the contrast and spatial resolution of these images is inferior to shadowgrahpy images it can provide valuable information on the nature of the ligaments seen in Figure 7. The structures are not visible on the diffuse light images. Instead a dense Schlieren system, most likely

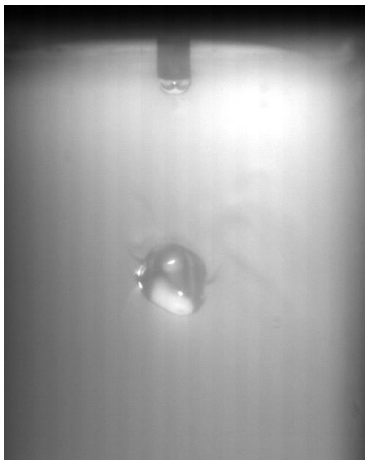

p_{ch} = 55 bar, T_{ch} = 528 K, T_{inj} = 453 K
Figure 8: Diffuse lighting method

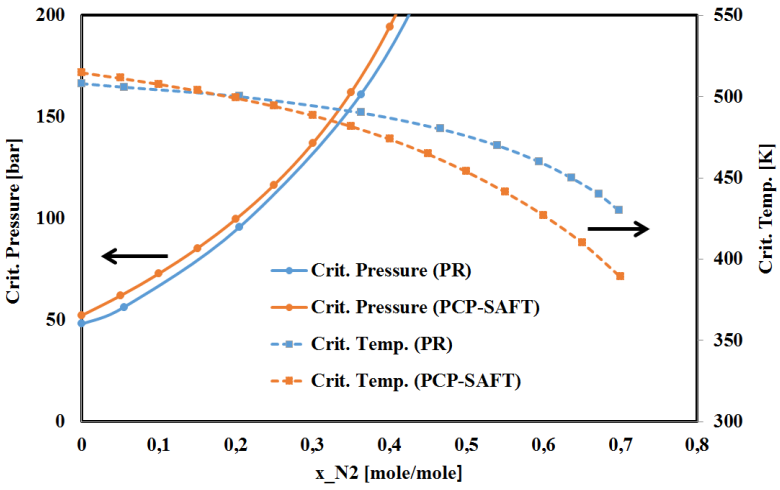

Figure 9: Critical mixing lines for acetone/nitrogen mixture

consisting of a dense acetone rich gas mixture, can be seen. Based on these findings the theory, that these ligaments consist of liquid acetone, can be refuted. The third analysis focused on thermodynamic properties of an acetone/nitrogen mixture. This work was performed in cooperation with the group of Prof. Vrabec, University Paderborn, and the group of Prof. Gross within the SFB-TRR 75. In Figure 9 data for the critical mixing line for an acetone/nitrogen mixture is presented. The first dataset (blue) was obtained numerically using the Peng-Robinson equation of state (PR-EOS) and the quadratic mixing rule. The parameters for the PR-EOS were validated experimentally in [14]. The second dataset (orange) was calculated with the PCP-SAFT equation of state [15, 16, 17]. For calculating the critical point of the mixture the approach of Heidemann & Khalil [18] was applied. The pure component parameters for the PCP-SAFT EOS are summarized in table 2. The binary interaction parameter k_{ij} = 0.0377 was adjusted to vapour-liquid data. The critical pressure and temperature for pure acetone are slightly overestimated.

Table 2 : The pure component parameters for the PCP-SAFT EOS

Species	Segment number m_i	Segment diameter σ_i [Å]	Segment energy parameter ε_i/k [K]	Dipole moment μ_i [D]	Quadrupolar moment $\|Q_i\|$ [DÅ]
nitrogen	1.1123	3.4212	92.397	-	1.5200
acetone	2.7993	3.2650	221.43	3.2255	-

While the critical temperature of the mixture acetone/nitrogen experiences only minor changes with increasing nitrogen mole fraction, the situation is different for the critical pressure. Already small amounts of nitrogen lead to a steep increase of critical pressure. This behaviour has major implications on the transition process of the droplet from sub- to supercritical state. The finger-like ligaments, which consist of an acetone rich gas mixture, presumably never reach a supercritical state due to the increase of the critical pressure of the mixture. Furthermore the composition of the acetone nitrogen mixture and the amount of nitrogen dissolved into the droplet plays a central role for the transition process of the droplet. If the mass diffusivity prevails over the thermal diffusivity, the droplet will most likely stay subcritical during its falling process. For this reason simulations of the transport properties in the vicinity of the critical point are currently ongoing, parallel to the experimental investigations presented here.
Summarizing the outcome of this study some important questions could be resolved: at the chosen supercritical conditions the droplet stays subcritical during the falling process, at least in the inner core. The finger-like ligaments most probably consist of a subcritical acetone rich gas mixture, due to the increase of the critical pressure of the mixture. The mass and thermal diffusion play a central role for the transition from sub- to supercritical state. The measurement of the droplet temperature and composition of the gaseous acetone/nitrogen mixture are in preparation and will complement the experimental campaign.

CONCLUSION

A combined approach to characterize the injection of acetone droplets into a nitrogen atmosphere from ambient to supercritical chamber conditions was presented. The chamber conditions were varied from 1 to 60 bar and 293 to 523K. The droplet was pre-heated up to 89% of the critical temperature. Strong oscillations during the falling process make it difficult

to calculate the evaporation rate and droplet size history. A novel 3D reconstruction method was introduced. The uncertainty of the droplet diameter calculation could be reduced from 0.26 to 0.045 mm. The accuracy can be further improved by reducing the FOV, which results in a better spatial resolution. A detailed analysis of the droplet disintegration process in the vicinity of the critical point was conducted. The oscillations during the falling process indicate the presence of surface tension even at supercritical chamber conditions. At the chosen conditions the droplet stays subcritical during its falling process, at least at the inner core. The finger-like ligaments, visible in the shadowgraphy images, consist most probably of an acetone rich gas mixture. The critical pressure of the mixture rises steeply with increasing nitrogen mole fraction. This effect hinders the transition from sub to supercritical state. For a more detailed understanding of the disintegration process measurements of the droplet temperature and the composition of the gaseous acetone/nitrogen mixture are necessary and planned.

ACKNOWLEDGEMENTS

The authors gratefully acknowledge the financial support by Deutsche Forschungsgemeinschaft trough the SFB-TRR75, project B2.

REFERENCES

[1] Bellan, J., Prog. Energy Combust. Sci., 26 (4-6), **2000**, p. 329
[2] Sato, J., Proc. 31st Aerospace Sciences Meeting, AIAA 93-0813, Reno, NV, **1993**
[3] Nomura, H., Ujiie, Y., Rath, H. J., Sato, J. and Kono, M., Proc. Combust. Inst., 26, **1996**, p. 1267
[4] Matlosz, R. L., Leipziger, S. and Torda, T.P., Int. J. Heat and Mass Tran., 15, **1972**, p. 831
[5] Savery, C.W., Juedes, D.L. and Borman, G.L., Ind. Eng. Chem. Fund. , 10(4), **1971,** p. 543
[6] Morin, C., Chauveau, C., Dagaut, P., Gokalp, I. and Cathonnet, M., Combust. Sci. Technol., 176(4), **2004,** p. 499
[7] Stengele, J., Prommersberger, K., Willmann, M. and Wittig, S., Int. J. Heat Mass Tran., 42(14), **1999**, p. 2683
[8] http://www.sfbtrr75.de/index.php/de/
[9] Oldenhof, E., Weckenmann, F., Lamanna, G., Weigand, B., Bork, B. and Dreizler, A., Prog. Propul. Phys., 4, **2013**, p. 257
[10] Weckenmann, F., Bork, B., Oldenhof, E., Lamanna, G., Weigand, B., Böhm, B. and Dreizler A., Z. Phys. Chem. , 225, **2011**, p. 1417
[11] Bork, B., Weckenmann, F., Lamanna, G., Weigand, B., Böhm, B. and Dreizler A., Proc. Spray 2012, Berlin, **2012**
[12] Lamanna, G., Kamoun, H., Arnold, B., Schlottke, K., Weigand, B. and Steelant, J., QIRT Journal, Vol.10, No.1, **2013**, p. 112
[13] Kim, S.J., Park, G.C., Nuc. Eng. Tech., Vol. 39(4), **2007**, p. 313
[14] Windmann, T., Köster, A. and Vrabec, J., J. Chem. Eng. Data, Vol. 57, **2012**, p. 1672
[15] Gross, J., Sadowski, G., Industrial & Engineering Chemistry and Research, 40, **2001**, 1244-1260.
[16] Gross, J., AIChE Journal, 51, **2005**, p. 2556
[17] Gross, J., Vrabec, J., AIChE Journal, 52, **2006**, p.1194
[18] Heidemann, R. A., Khalil, A. M., AIChE Journal, 26, **1988**, p.769